AD 295 052

63-2-3

295 052

THE DEVELOPMENT OF AN AUXILIARY ELECTRODE THERMIONIC CONVERTER

FOURTH QUARTERLY TECHNICAL REPORT

JANUARY 1963

PREPARED FOR

FLIGHT ACCESSORIES LABORATORY
AERONAUTICAL SYSTEMS DIVISION
AIR FORCE SYSTEMS COMMAND
WRIGHT PATTERSON AIR FORCE BASE
OHIO

PROJECT 8173

TASK NO. 817305-9

(PREPARED UNDER CONTRACT AF33(657)-8005)

PREPARED BY

RADIO CORPORATION OF AMERICA
ELECTRON TUBE DIVISION
LANCASTER, PENNSYLVANIA

AUTHORS W.B.HALL AND J.J. O'GRADY

THE DEVELOPMENT OF AN AUXILIARY ELECTRODE THERMIONIC CONVERTER

FOURTH QUARTERLY TECHNICAL REPORT

JANUARY 1963

PREPARED FOR

FLIGHT ACCESSORIES LABORATORY
AERONAUTICAL SYSTEMS DIVISION
AIR FORCE SYSTEMS COMMAND
WRIGHT PATTERSON AIR FORCE BASE
OHIO

PROJECT 8173

TASK NO. 817305-9

(PREPARED UNDER CONTRACT AF33(657)-8005)

PREPARED BY
RADIO CORPORATION OF AMERICA
ELECTRON TUBE DIVISION
LANCASTER, PENNSYLVANIA

AUTHORS W.B. HALL AND J. J. O'GRADY

FOREWORD

This report was prepared by the Radio Corporation of America on Air Force Contract AF33(657)-8005 under Task Number 817305-9 of Project Number 8173, "The Development of an Auxiliary Electrode Thermionic Converter". The work is being administered under the direction of the Flight Accessories Laboratory, Aeronuatical Systems Division, Lt. D. Raspet is Project Engineer for the Laboratory.

The report covers the work applied, from 15 September 1962 to 15 December 1962, and represents the efforts of Thermionic Converter Engineering of Power Tube Operations, RCA-Lancaster. W. B. Hall is the Engineering Leader responsible for the technical direction and control of the project under the direct supervision of F. G. Block, Manager.

This report is the Fourth Quarterly Technical Report for the subject contract.

This report is unclassified.

> "The work covered by this report was accomplished under Air Force Contract AF33(657)-8005, but this report is being published and distributed prior to Air Force review. The publication of this report, therefore, does not constitute approval by the Air Force of the findings or conclusions contained herein. It is published for the exchange and stimulation of ideas".

ABSTRACT

This report covers the fourth three-month period of effort under a thirteen-month program to improve the efficiency and life expectancy of thermionic energy converters for space applications.

The program has been modified to the development of a cylindrical converter, the emitter of which is thermally bonded to but electrically insulated from a central heat-source tubing carrying liquid metal.

Significant progress has been achieved in the various portions of the program. A particular geometry employing the "Cross-Current Converter" principle was selected and the overall design has been determined. Two promising methods for the application of the emitter insulation are being evaluated. The effects of cesium on ceramics at the various temperatures of interest were observed and the results analyzed.

FOURTH QUARTERLY TECHNICAL REPORT
CONTRACT AF33(657)-8005

THE DEVELOPMENT OF AN AUXILIARY
ELECTRODE THERMIONIC CONVERTER

TABLE OF CONTENTS

LIST OF ILLUSTRATIONS

LIST OF ILLUSTRATIONS
(Continued)

LIST OF TABLES

FOURTH QUARTERLY TECHNICAL REPORT
CONTRACT AF33(657)-8005

THE DEVELOPMENT OF AN AUXILIARY
ELECTRODE THERMIONIC CONVERTER

SECTION I

INTRODUCTION

The effort under the subject contract is a continuation of the work done under Air Force Contract AF33(616)-7903 and consists of the continued modification and improvement of converters determined most promising under that contract.

In order to demonstrate compliance with the program objective RCA was directed to design, fabricate, test and deliver one "Six-Volt Generator". Modification 1 to the subject contract, with an effective date of 10 September 1962, deletes this requirement and substitutes a cylindrical converter installed upon a center heat-source tubing of columbium, one percent zirconium, and insulated therefrom by aluminum oxide.

In view of the above, RCA has cancelled its program for the "Six-Volt Generator" and in its place plans the following program.

* *

Manuscript released by the author 28 December 1962 for publication as an ASD Technical Documentary Report.

31 December 1962

RCA will investigate potentially suitable means of applying electrical insulation between columbium - one percent zirconium tubing and cylindrical refractory thermionic emitters. RCA will restrict the scope of this effort to the insulator Aluminum Oxide (Al_2O_3) and application techniques such as flame spraying, vapor deposition, etc., insofar as they apply to that material.

RCA will accomplish analysis, conceptual design, experimental fabrication, operation and evaluation of a laboratory model of a cylindrical thermionic converter the emitter of which is mounted integrally on, but electrically insulated from, a coaxial tubulation suitable for installation and operation on a test loop carrying flowing, heated liquid metal (e.g. lithium). RCA will demonstrate successful operation of such a converter by means of electrical test heating. Thermionic performance of the converter will be demonstrated by rated output voltage and current at design temperature. Insulation performance will be demonstrated by adequate electrical resistivity of the insulation under test conditions corresponding to rated converter output.

The delivery of this unit will be accomplished by 15 February 1963.

This report covers the effort applied during the Fourth Quarterly Report period, 15 September 1962 through 15 December 1962.

SECTION II
SUMMARY

The program has progressed to the point where the particular electrode geometry can be selected based upon the research and development accomplished. This selection, designated the "Saw Tooth Design" employs the "Cross-Current Converter" principle to increase current density and at the same time overcome mechanical disadvantages of other designs.

The prototype converter, to satisfy Modification 1 of the contract, has been designed to meet all the objectives of the program. Determinations regarding the particulars of the various component designs, the processing jigs and techniques, the test fixtures and procedures and the converter test program have been largely completed. All component parts were ordered and received.

In order to assure satisfactory insulation of the emitter from the heat source, two methods for applying the insulation are being investigated: plasma spraying of aluminum oxide; and casting of pure aluminum oxide (sapphire).

The effects on ceramics of cesium liquid at 370° Centigrade and cesium vapor at test temperatures of 370°, 750° and 1200° Centigrade have been determined.

SECTION III

DETAILED FACTUAL DATA

A General

Progress has been made in the various portions of the program during the past quarter. The electrode geometry was selected for use in the insulated converter. Converter processing techniques were resolved. The complete design was reviewed, modified and fabrication started. Two methods for insulating the emitter from the heat source show promise and are being evaluated. The cesium compatibility tests are nearing completion.

B Geometry Selection

The related series of converters for the subject contract employs the basic principle of the "Cross-Current Converter". This approach enhances the ionization through an increase in current density which in turn further increases the current density and the useful power density.

1. Theory

The theoretical principles on which the program was based, and the method by which each of the various geometries utilize these principles were included in the Second Quarterly Technical Report, pages 8, 9, 10, 11, 12 and 13.

The theory, in condensed form, states that the ionization efficiency is increased as the current density within the same gap volume is increased. Hence, if the ionization efficiency is increased, more ions will be available to neutralize the space charge, thus causing emitted current density and the power density to increase further.

2. Data

All geometries employed under the subject contract, with the exception of the planar configuration, were designed to increase the current density

in the same gap volume and therefore employ the "Cross-Current" theory. The "Auxiliary Electrode Design" and the "Dual Converter Design" were undertaken in order to prove the theory. The "Auxiliary Electrode Design" employed an auxiliary collector which was operated at different load conditions from the main collector. This operation increased the current density within the gap between the emitter and the auxiliary collector. The increase in ionization efficiency in the auxiliary section created excess ions which then diffused into the main converter section. The rate of diffusion of ions was found to be too slow to give a substantial increase in power output in the main converter. The dual converter overcomes this problem by obtaining a higher current density in the same gap volume making it unnecessary for the ions to diffuse. The current density in the "Dual Converter Design" gap volume was varied widely by controlling the current drawn across the auxiliary converter. The effect on the main converter performance showed conclusively that the theory is sound. How the converter improves by increasing current density from an auxiliary source is seen from the data presented in the Third Quarterly Technical Report, pages 19 and 20.

3. Evaluation

The "Box Design" and the "Saw-Tooth Design" are identical with respect to the interaction that takes place within the gap, and the means by which this interaction is accomplished. A large scale drawing of these designs is shown as Figure 1. Both designs have surfaces on the emitter that are ninety degrees from each other, from which electrons enter the gap within the same volume. Opposite the emitter surfaces are equivalent collector surfaces which are spaced from the emitter at the optimum distance. Since electrons are emitted from two surfaces at ninety degrees, the current density within the gap is approximately doubled, thus causing an increase in the ionization efficiency. An increase in current caused by increased ionization efficiency further enhances the converter operation.

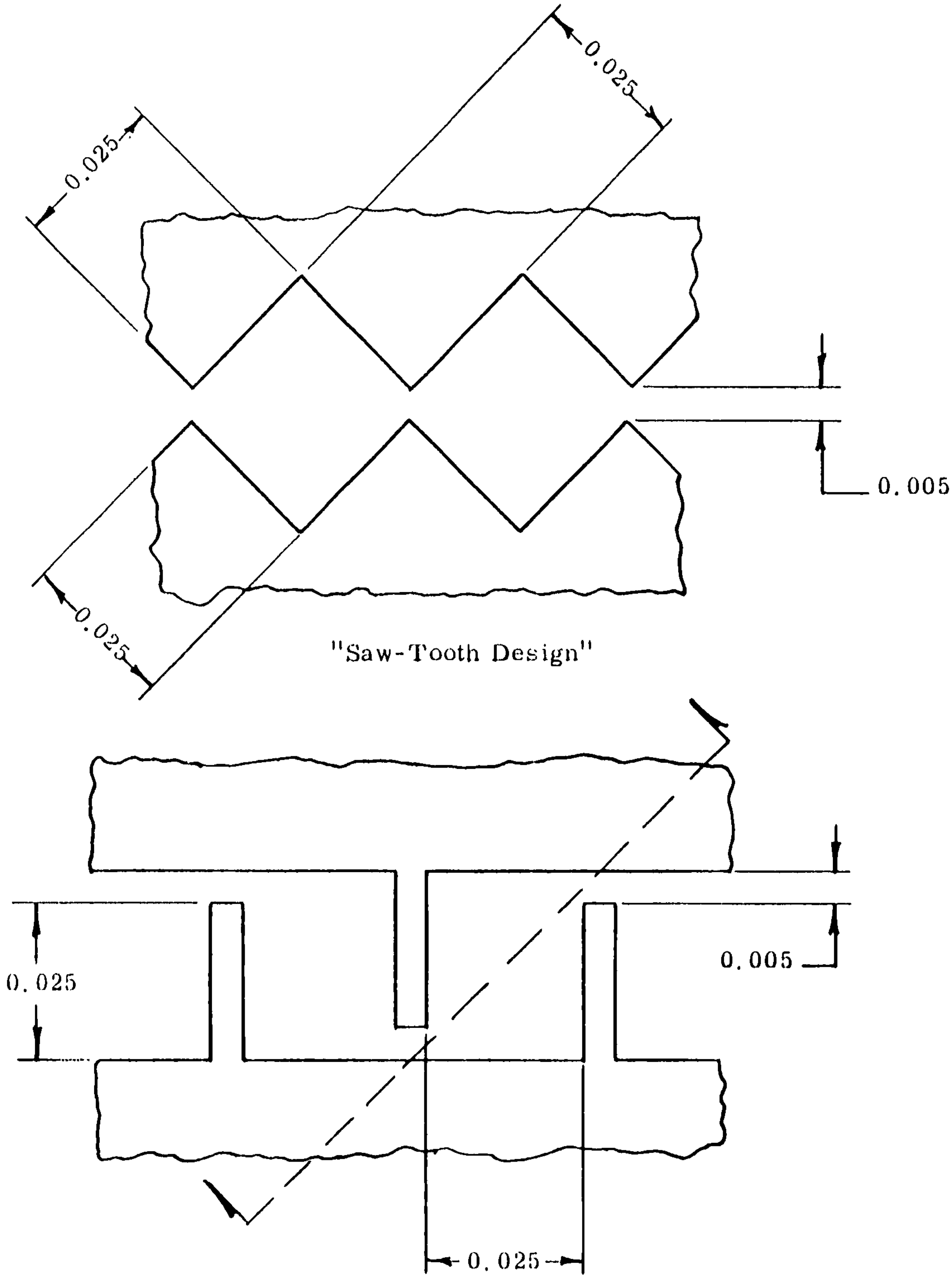

FIGURE 1 - LARGE SCALE DRAWING SHOWING COMPARISON OF "SAW TOOTH" AND "BOX" DESIGNS

Both of these designs should, theoretically, give the same performance. However, the "Box Design" has certain disadvantages which are overcome by the "Saw-Tooth Design". Electrode temperature cannot be maintained with the required uniformity in the "Box Design" since each rib on the emitter and collector is too thin to conduct the required heat flux. If the ribs were made thicker to obtain better temperature uniformity, the end of the rib becomes a significant part of the emitter area and is spaced too close to the collector to allow "ball-of-fire" operation from this area at less than 1500° Kelvin. The "Saw-Tooth Design" overcomes both of these disadvantages.

During the program many process changes were made which enhanced converter operation. In order that improvements in converter performance, which were made by the above changes in geometry, could be distinguished from those caused by processing changes, the planar converter performance was used as a standard throughout the program against which the converters of other geometries could be compared.

4. Conclusion

In view of the above, RCA has selected the "Saw-Tooth" geometry for incorporation into the converter to be delivered under the subject contract. This decision was based upon the results obtained with both the "Box Design" and the "Saw-Tooth Design". The selected geometry will be used in the A-1194B converter type for further evaluation.

In order to facilitate the program, it is planned to build initial samples of the insulated cylindrical converter for liquid-metal heating with a plane cylindrical geometry to verify the mechanical and thermodynamic design. After assurance of satisfactory performance is obtained, the "Saw-Tooth" geometry will be incorporated.

A cross-sectional drawing of the proposed RCA Developmental Converter Type A-1198B, is included as Figure 2.

C Experimental Converters

In order to resolve the processing techniques sixteen converters were fabricated and tested. This series of units included seven having "Saw-Tooth" emitter geometry and nine of planar configuration.

The liquid helium freeze-out procedure was employed to substantiate the data obtained in the previous Quarterly Report period. However, low-power output caused by other parameters resulted in inconclusive results. The low-power output was found to be caused by imperfect cesium capsule processing.

Two converters employing "Saw-Tooth" geometry were fabricated with identical parts and processed, using identical procedures except for the bakeout temperature of the cesium capsule. Remarkably different results were obtained as can be seen from the data presented in Figure 3. The cesium capsule used in Converter Serial Number 82C, was baked at 450° Centigrade for six hours compared to that used in Converter Serial Number 83C, which was baked at 300° Centigrade for six hours. Cesium attack on the copper capsule during bakeout is probably the cause of the low-power output on Converter Serial Number 82C. Other converters processed similar to Converter Serial Number 82C also gave poor results. Previous converters which employed liquid helium freeze-out had been processed at the higher capsule bakeout temperatures causing both capsules to be affected. These data explain the sporadic results previously obtained.

Pertinent data for the evaluation of the curves of Figure 3 are detailed below in Table I.

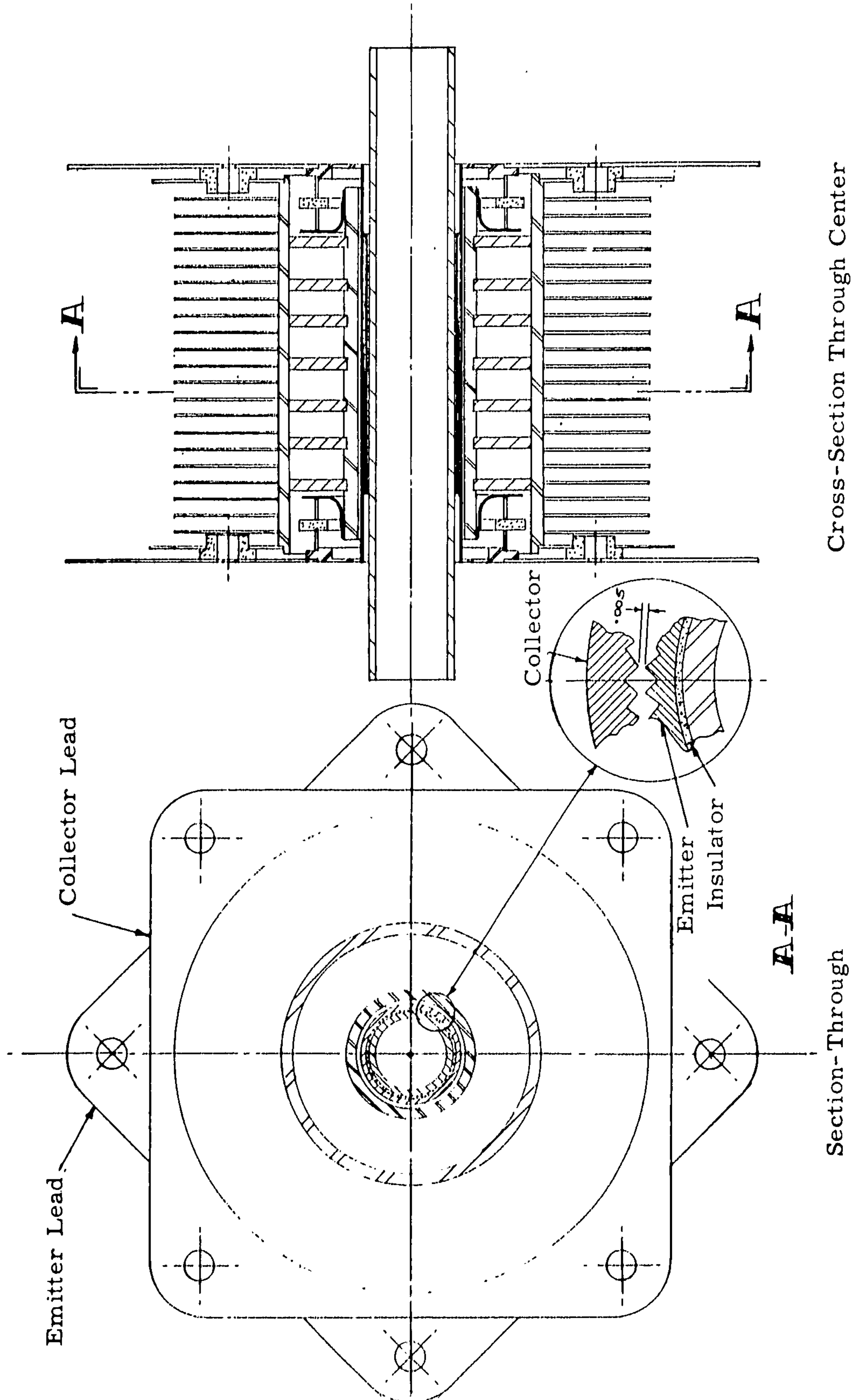

FIGURE 2 - RCA DEVELOPMENTAL CONVERTER TYPE A-1198B

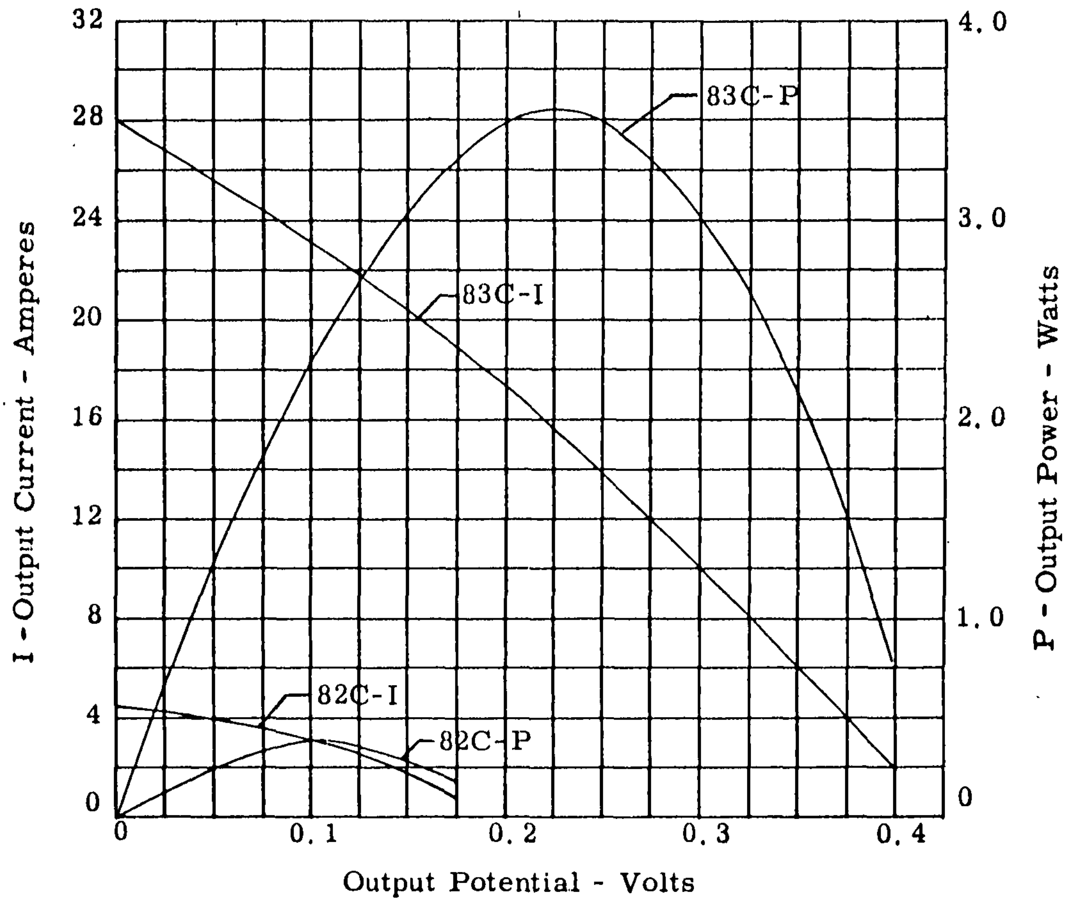

FIGURE 3 - OUTPUT CHARACTERISTICS OF CONVERTERS
SERIAL NUMBERS 82C AND 83C

TABLE I

TEMPERATURE DATA

	Converter Serial Number 82C	83C
Emitter Temperature °Centigrade	1180	1185
Collector Temperature °Centigrade	515	525
Cesium Temperature °Centigrade	285	275
Cesium Capsule Batch	#20	#20
Total Projected Emitter Area Cm^2	2. 4	2. 4
Effective Emitter Area Cm^2	3. 5	3. 5
Emitter Geometry	Saw-Tooth	Saw-Tooth
Cesium Capsule Processing Temperature °Centigrade	450	300

D Insulated Converter

In order to comply with Modification 1 of the subject contract, a new converter design designated RCA Developmental Converter A-1198B was developed. The overall design of the converter embodies the latest advancements for achieving the objectives of the program. The emitter is electrically insulated but thermally bonded to the liquid metal heat source. The inner heat source tubing is columbium, one percent zirconium. The emitter and collector surfaces are designed in the "Saw-Tooth" geometry as shown in Figure 1.

1. Converter Design Considerations

Limited by a maximum operating temperature of 1500° Kelvin, power output in excess of one watt per square centimeter can be attained based on the performance record of the A-1194B thermionic converter. The designed emitter area of 40 square centimeters will result in a power output in excess of 40 watts. The output characteristics at optimum operation was designed to be approximately 200 amperes at 0. 2 volt.

Since the converter is designed to operate in a vacuum, conduction and convection as a means of heat transfer cannot be used to dissipate waste

heat. Therefore, heat dissipation from the collector depends solely on radiation as follows:

$$W = \epsilon \sigma (T_1^4 - T_2^4)$$

where

W = Heat radiated in watts

ϵ = Emissivity

σ = Sephan Boltzmann constant

T = Temperature in degrees Kelvin

Once the heat flux to be radiated and the operating temperature of the surface of the collector is determined, the design of the radiator depends on those factors which will achieve minimum weight as an objective.

The theoretical evaluation of several prototypes proved a need for fin radiators, but that if fins were attached directly to the collector the length and weight would be excessive. Since the temperature drop along a thin copper fin is not negligible, and radiation is governed by the fourth power of the radiating temperature, the fin length and thickness becomes critical to assure the highest radiating temperature with minimum weight. The design of the radiator can be seen in Figure 2. Seven copper supports, 0. 100 inch thick spaced along the collector were brazed to the collector O. D. These supports were then enclosed in a copper cylinder to which the fins were brazed.

The initial design was developed with a non-insulated emitter to permit the simplest fabrication while resolving the design of jigs, fixtures and brazing schedules. The non-insulated version employed a planar surface geometry but was similar in overall dimension and basic assembly

to the insulated design. The basic design incorporates two tubes of molybdenum with the inner tubing nickel plated in the region of contact with the outer. This assembly was brazed in a vacuum furnace at 1350° Centigrade for two hours causing a Nickel-Molybdenum eutectic braze to be formed.

Cesium compatibility was a necessary factor in determining the converter materials. Brazing techniques are being investigated to permit the use of Nickel-Molybdenum and Nickel-Niobium brazing materials. Current converters employ gold copper brazing alloys.

2. Electrical Heater Design Considerations

An electrical heater to simulate liquid-metal heating and capable of reliable operation must be designed within certain parameters. It must transfer the required power to the emitter at a low enough operating temperature to give long reliable life. It must maintain the correct emitter operating temperature with uniformity over the emitter length. Compensation for the end losses in a radiation type heater can be achieved by reducing the cross section of the heater in this area to produce uniform emitter temperature. The design of the heater is shown in Figure 4.

3. Jigs and Fixtures

Since high-temperature brazing alloys are being employed in the converter design, the jiging fixtures were designed with materials that would not form alloys with the converter parts at processing temperatures.

The ceramic seal assembly jig and the emitter collector assembly jig employ ceramic inserts to separate the metal parts of the jigs from

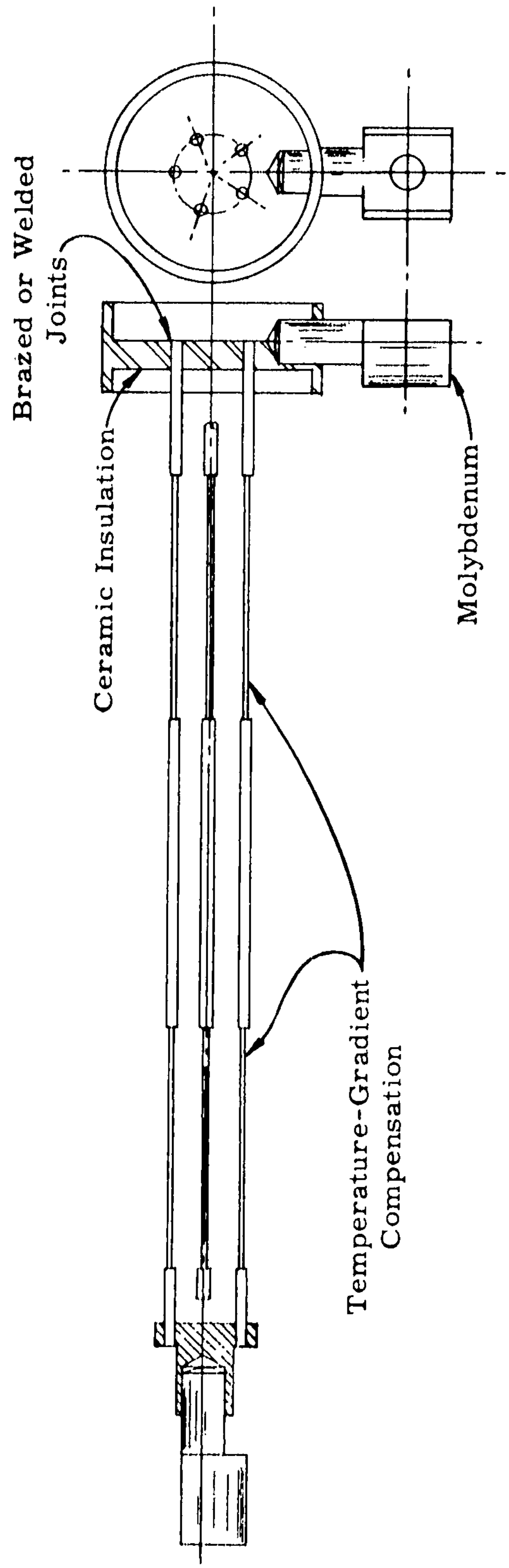

FIGURE 4 - HEATER DESIGN - WELDED ASSEMBLY

those of the assembly. These inserts can be seen in Figures 5 and 6. Both solid ceramic and plasma-sprayed ceramic bodies are used.

4. Test and Evaluation

a. Heater Test

The heater test was designed so that the heater temperature and the uniformity of the emitter temperature could be accurately determined. A dummy emitter made of niobium was used for the test. Holes were drilled through the emitter so that the heater temperature could be measured with an optical pyrometer and thermocouples for emitter temperature measurement were attached at three places along the emitter. The placement of these bodies and thermocouples can be seen in Figure 7. The thermocouples were placed at the middle and at each end of the active emitter area in order to determine the temperature uniformity. Since the dummy emitter has a lower heat loss pattern than an active converter the test was conducted at higher temperatures than those employed in typical converter operation. In addition, a converter will lose substantially more heat through the ends due to electrical lead connections. Thus the temperature test on a dummy emitter will show a temperature higher at each end than in the middle for uniform temperature distribution to be achieved in the final converter.

Two heaters were tested, one of brazed construction and the other of welded construction. It was observed that the brazed construction would not withstand the temperature required. Additional end compensation was used in the welded construction. A comparison of the data shown in Figure 8 and Table II shows that the welded heater requires less power to obtain the same emitter temperature and that the additional end compensation of the welded heater has improved the emitter temperature uniformity. The temperature of

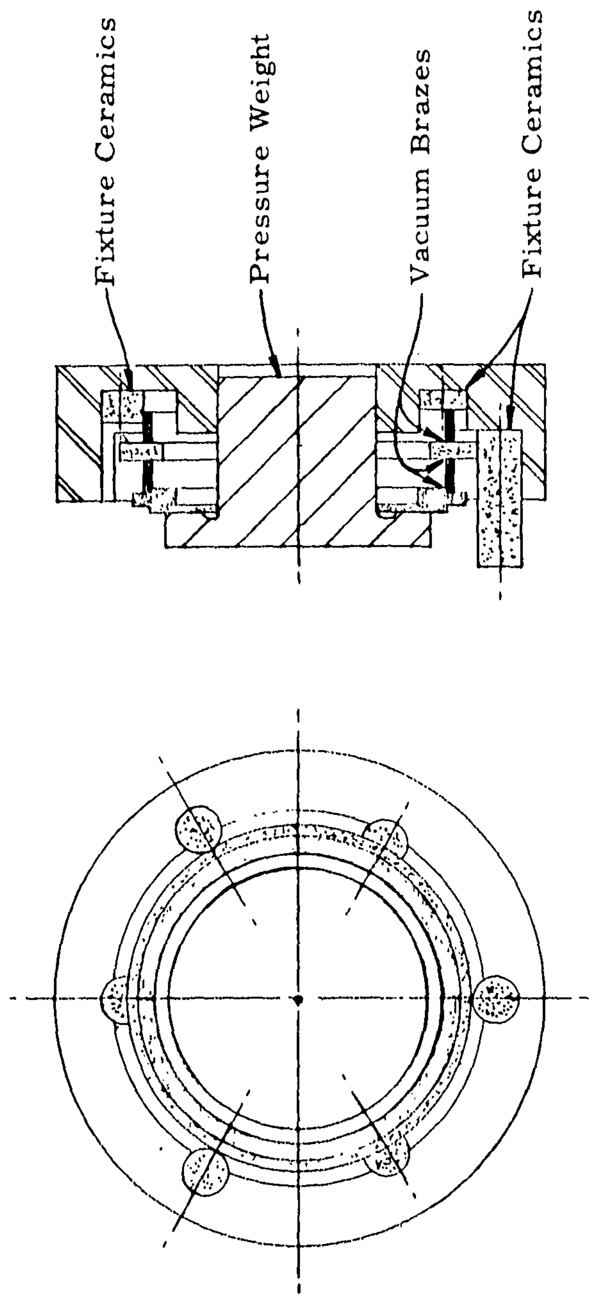

FIGURE 5 - SEAL-ASSEMBLY FABRICATION FIXTURE

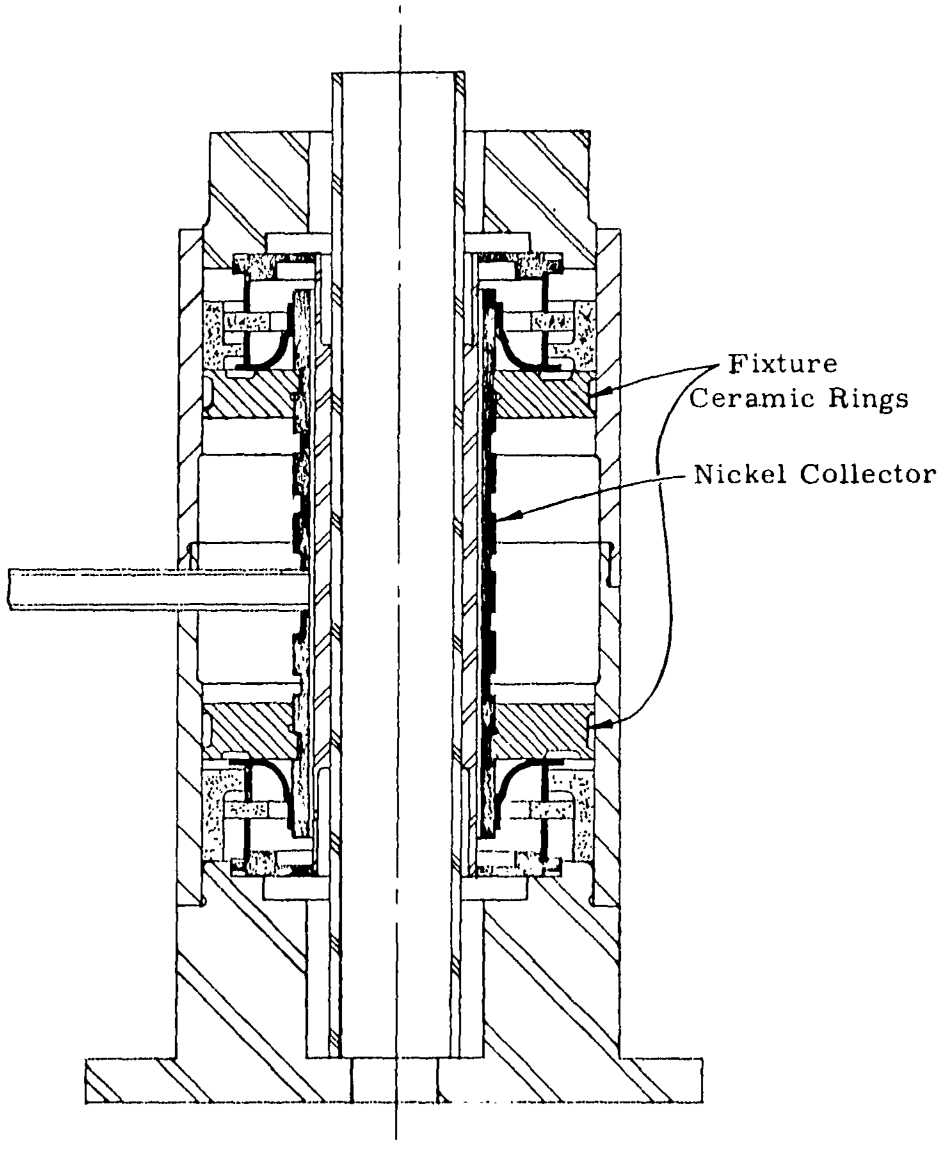

FIGURE 6 - EMITTER-COLLECTOR-ASSEMBLY FABRICATION FIXTURE

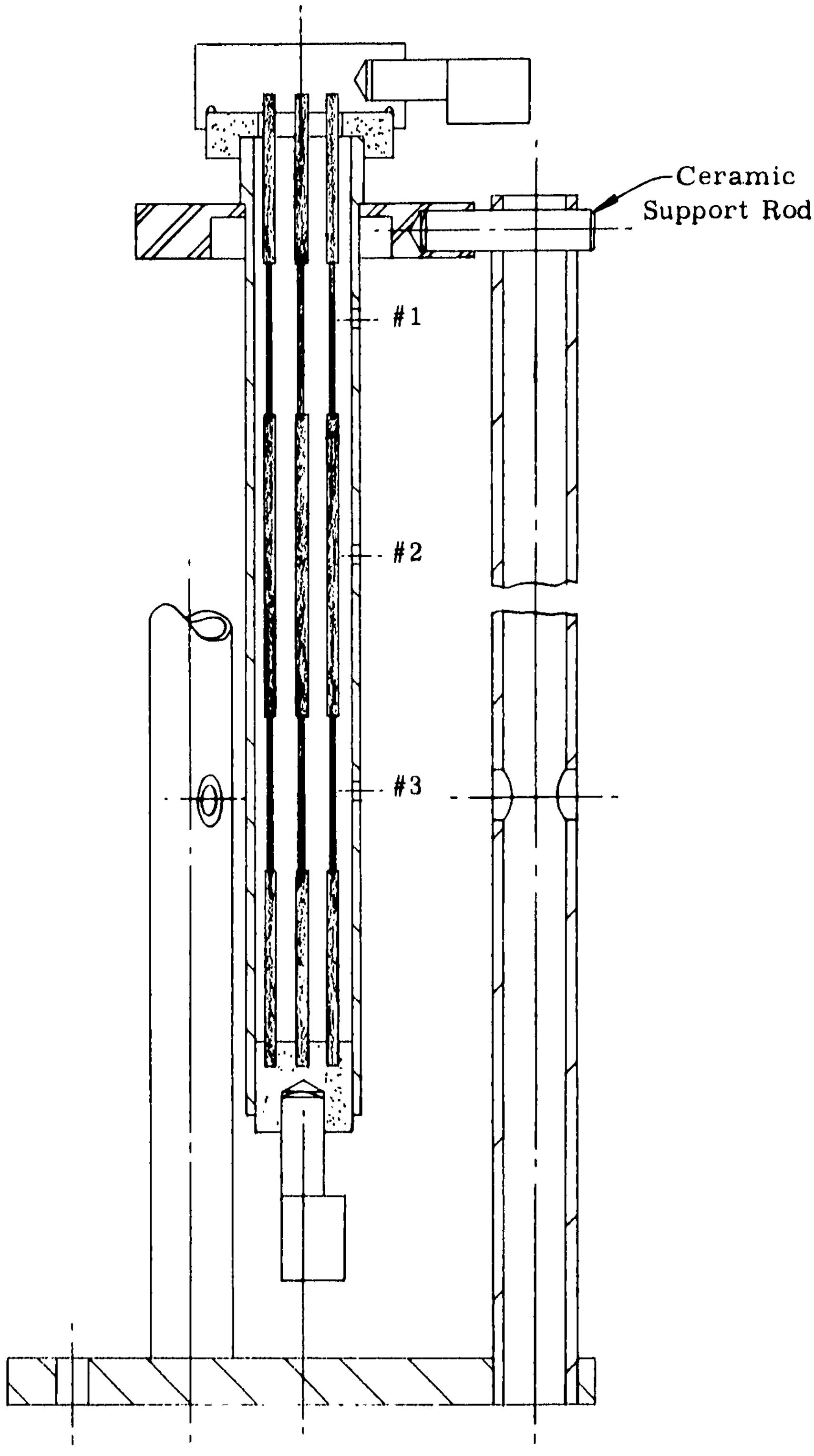

FIGURE 7 - HEATER EVALUATION TEST SET-UP

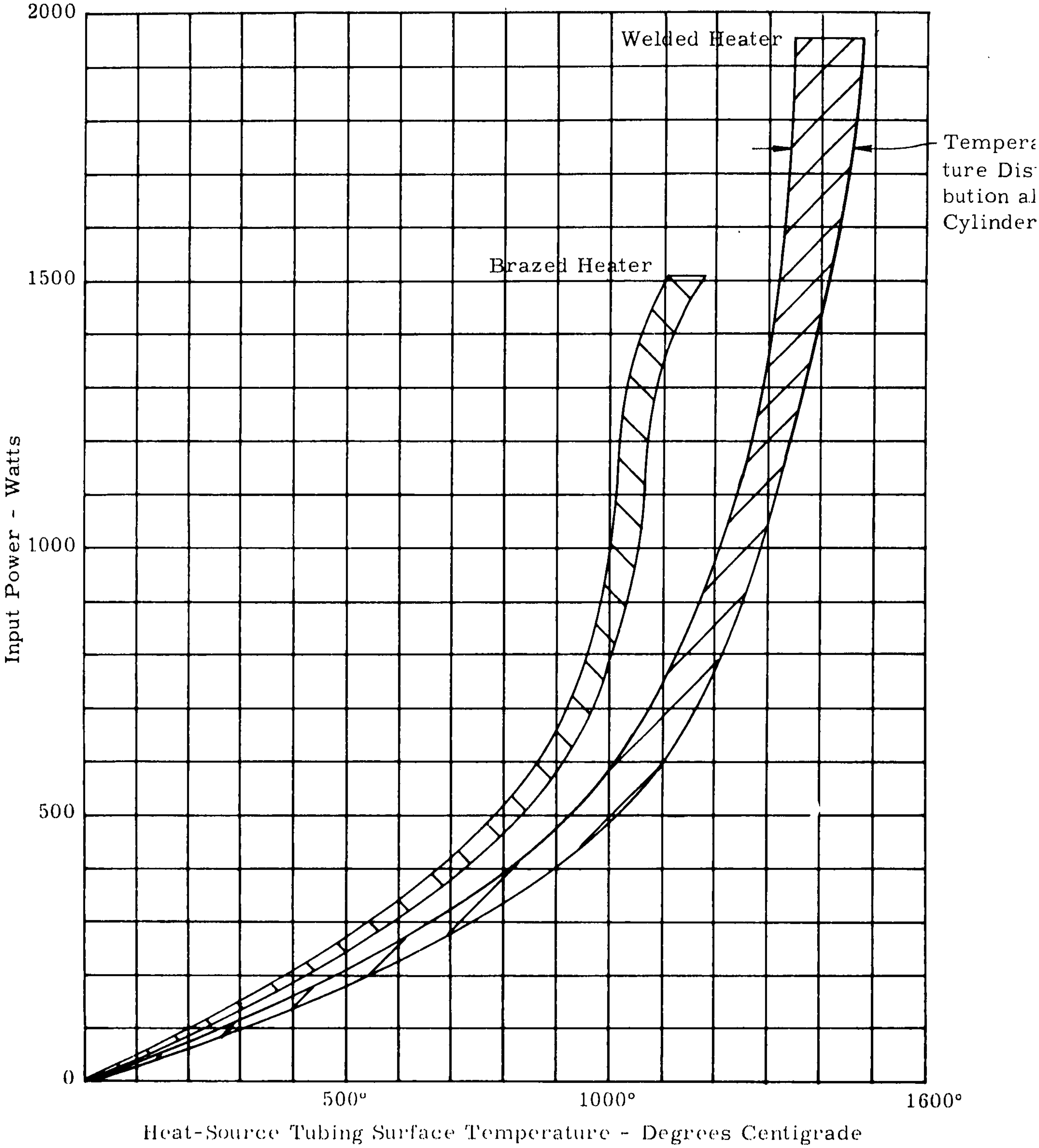

FIGURE 8 - COMPARISON OF BRAZED VERSUS WELDED HEATER ASSEMBLIES

TABLE II

TEMPERATURE DISTRIBUTION ALONG HEATER ASSEMBLY

	I Amperes	E Volts	Thermocouple °C #1	Thermocouple °C #2	Thermocouple °C #3	Filament Temperature °C #1	Filament Temperature °C #2	Filament Temperature °C #3
1.	Brazed Construction							
	275	2.7	940	990	970	1625	1535	1605
	300	4.2	1020	1080	1060	1745	1660	1740
	325	4.6	1100	1170	1150	1910	1750	1905
2.	Welded Construction							
	250	2.3	990	1090	1090	1615	1555	1605
	300	4.0	1170	1250	1240	1905	1705	1905
	350	5.6	1350	1460	1480	2110	2055	2115

Thermocouple Number 1 is lower than that of Number 3 because heat is drained away from the area of Number 1 by the holding fixture. It can be seen in Table II that the end temperature Number 3 is hotter than the center temperature Number 2. This is the desired effect. Additional heater compensation will be employed to correct the excessive difference in temperature between thermocouple points Numbers 1 and 2. The additional end loss at point Number 1 closely simulates the end loss in an actual converter.

b. Radiator Test

A radiator test is currently being scheduled. The test will determine the radiator capability of dissipating the required heat flux at the desired collector temperature during typical converter operation. The radiated heat will be measured calorimetrically while the collector temperature is observed. A curve of radiated power versus collector temperature will be taken and the data compared with the desired operating conditions. The design of the test position is shown in Figure 9. The radiator is enclosed in a water-cooled absorber from which the heat radiated from the converter can be measured.

c. Emitter Test

A special test fixture (see Figure 10) will be used for the emitter test. This test will compare the heat transfer characteristics of the insulated and non-insulated emitters. Test procedure: two points on each assembly, labeled A_1 and A_2, on Figure 10 on the columbium tube, will be held constant for all tests. These locations will be reference points. The emitter surface temperature will be observed at three locations (B_1, B_2 and B_3) along its length. A comparison of the temperature differential between

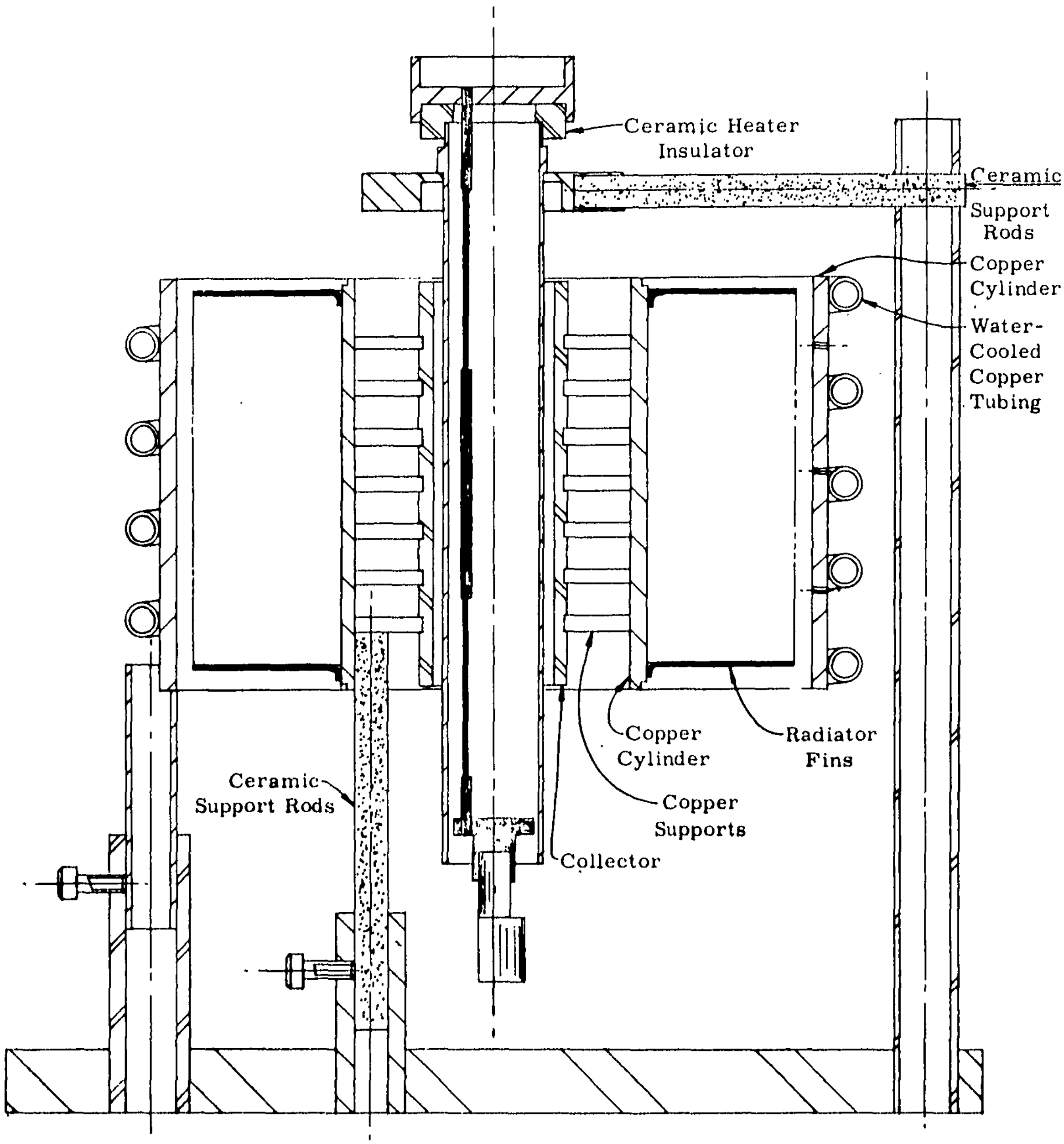

FIGURE 9 - FIN-RADIATOR TEST FIXTURE

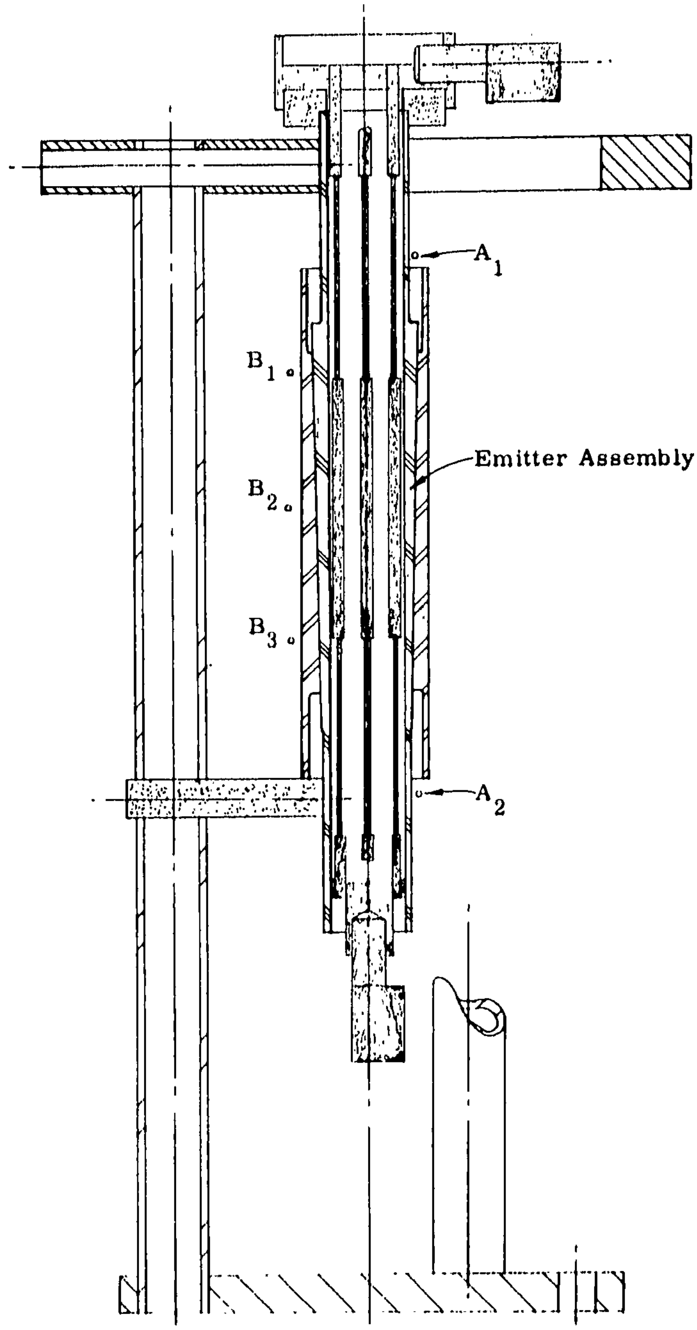

FIGURE 10 - TEST FIXTURE FOR TEMPERATURE GRADIENT OF EMITTER ASSEMBLY

either one of points A_1 and A_2 on the heat source tubing with the temperature of the emitter at any one of points B_1, B_2 and B_3 for both the insulated and non-insulated assemblies will be made. This information will give an accurate measurement of the temperature drop across the emitter insulation with the required heat flux.

d. Converter Test

The overall converter will be tested in a set-up as shown in Figure 11. The converter will be energized and brought to operating conditions to observe output characteristics. In order to prevent deterioration of performance the converter will be decesiated and any contaminants removed. A second cesium capsule will be employed to reactivate the unit. The unit will be continually adjusted for optimum operation until stable temperature conditions are achieved. The heat loss from the heater leads and losses through the ends of the converter will be measured calorimetrically. This information will permit the accurate measurement of converter efficiency.

E Insulated Emitter

The major emphasis in the area of materials and processing was directed toward achieving an emitter, electrically insulated from the center heat-source tubing but bonded thermally to it to obtain good heat transfer. Three basic designs were considered.

1. Vapor Deposition

The first design employed a process of depositing an insulator on the columbium tubing by reducing a metal halogen and oxidizing it at the same time. The emitter was then added by vapor deposition by the reduction of molybdenum chloride with hydrogen. This method appeared feasible but the time required for optimizing the required techniques prevented a timely solution. In addition, the characteristics of the

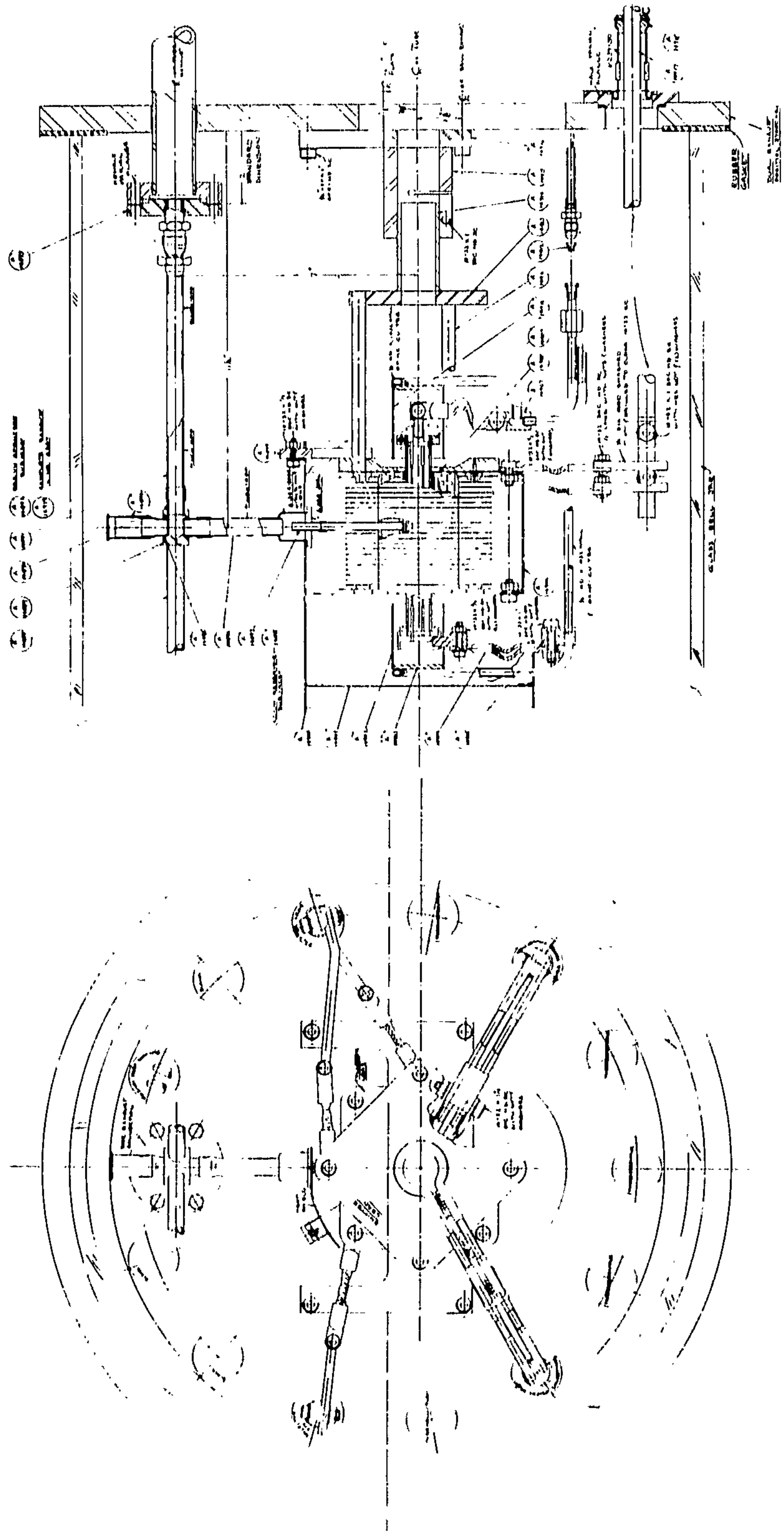

FIGURE 11 - CONVERTER TEST POSITION

deposit as an emitter were uncertain. Because of these reasons, the process was dropped.

2. Plasma Spraying

The second technique was plasma spraying of alumina onto the tube and then applying the emitter by shrink fitting or growth through vapor deposition. The latter technique was given up early for reasons mentioned above. Shrink fitting developed into two variations which are being tried as method A and B. The assembly is essentially a columbium tube machined over an area slightly longer than the planned emitting length. Onto this area seven to nine mils of alumina was plasma sprayed and ground to a design thickness of 5 mils. A second columbium tube was then machined on its I. D. to match the first tube. These two tubes were then fused together at 1500° Centigrade. To assemble the emitter with its leads to the columbium subassembly it was designed so that the O. D. of the outer columbium tube was nickel plated and brazed to the I. D. of the molybdenum emitter at 1350° Centigrade. The force applied to the brazed joint would result because the expansion of columbium is slightly greater than molybdenum. The main advantage of this method is its extremely close match in thermal expansion of the components. At 1200° Centigrade there is only a mismatch of 1-3/4 mils per inch and it is compressive because of the nature of the design. Its main disadvantage is that columbium is a reactive metal and might have a tendency to reduce the alumina during the long-life expectancy of the converter.

The second variation of this technique was to plasma spray alumina onto a molybdenum tube and grind the alumina to 5 mil thickness. A second molybdenum tube using the O. D. as the emitting surface and having an I. D. machined to match the first tube was fused to the plasma sprayed alumina at 1500° Centigrade. This subassembly was then brazed with nickel to the O. D. of a columbium tube. To date, an emitter assembly

has been made to this variation and test equipment is being readied to evaluate its heat transfer characteristics. This will be done by duplicating an earlier described set-up for the non-insulated version and comparing the surface temperature profile of the emitter at a given power input. The difference in temperature can be accounted for by the interlaying layer of alumina. At the same time the assembly will be heat cycled to observe any structural faults.

The disadvantage of this variation is the poorer match of coefficient of expansion of the molybdenum to the alumina. At 1200° Centigrade there is a mismatch of 2-1/4 mils per inch with the stresses being tensile rather than compressive as in the first variation. Its advantage is that there is no chemical reactions between the molybdenum and alumina which might lead to the degradation of the insulation.

The plasma spray techniques also have the disadvantage that the density of the alumina is only 85 to 90 percent of its theoretical value which means its heat transfer characteristic may be reduced to a similar degree. To overcome this disadvantage, a third technique was developed which incorporated casting sapphire between two walls of coaxial pipes of molybdenum.

3. Casting

The casting process has been designated Method C and the cast assembly is sketched in Figure 12. The casting is done by melting sapphire at 2200° Centigrade in a hydrogen atmosphere and letting the liquid run down between the walls of the tube. Enough sapphire is melted to insure complete filling. The cast assembly is then machined to the structure illustrated in Figure 13 and a columbium tube is nickel brazed to its I. D. to complete the emitter assembly. The disadvantage of this technique is that the final assembly is extremely difficult to machine. To

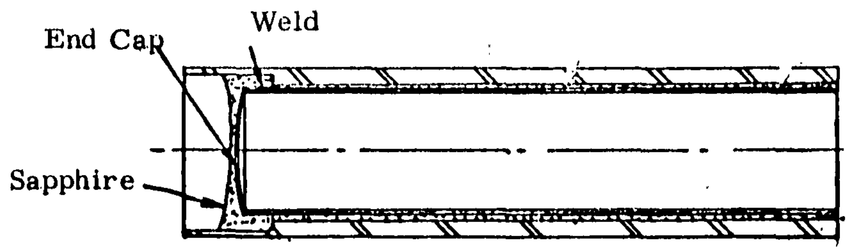

Cast Assembly

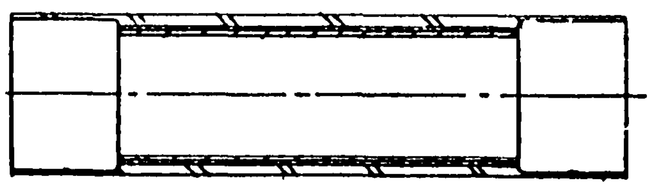

Finish Machined Assembly

FIGURE 12 - THE STEPS IN MELTING ALUMINUM OXIDE

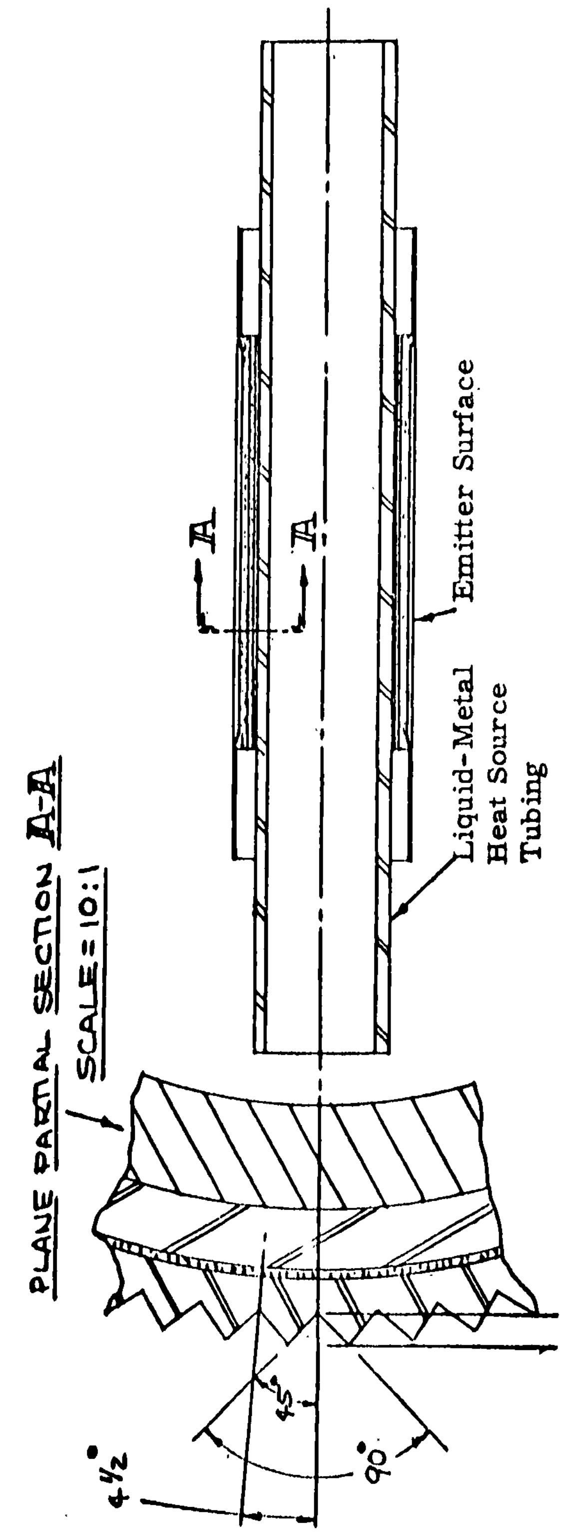

FIGURE 13 - ALUMINUM OXIDE MELTED BETWEEN MOLYBDENUM TUBING - METHOD C

date, two out of three assemblies have developed cracks in the recrystallized molybdenum during machining. Its second disadvantage is the short surface leakage path, 5 mils, compared to a possible 1/4 inch for the plasma technique. Upon completion of the test position, the heat transfer characteristics of this structure will be compared to that of the plasma-sprayed alumina design and the non-insulated version. It will also be temperature cycled to observe structural faults which may lead to premature failure.

Besides evaluating the heat transfer of the various designs and temperature cycling, it is also planned to measure the electrical resistance as a function of temperature for the two techniques being developed and also evaluate the bond between the members by cross-sectioning and by ultrasonic flaw detection.

In preliminary tests of the resistance of the plasma-sprayed alumina, 0.005 inch of alumina was sprayed on a molybdenum tube approximately 0.700 inch diameter by 1.5 inches long. Then molybdenum was plasma sprayed over the alumina to form a structure similar to a capacitor. Contacts were made to I. D. and O. D. and a resistance of 3×10^6 ohms was measured at room temperature and 8.7×10^2 ohms at 1260° Centigrade in hydrogen. The resistance was measured by applying 20.0 volts across the alumina and measuring the current flow. The resistance did not change during a test of two hours at 1260° Centigrade. A photomicrograph of the structure tested is shown in Figure 14. The alumina was in very intimate contact with the molybdenum surface and appeared to be very dense.

A cross section of a cast sapphire structure is shown in Figure 15. Again, the structure of sapphire was very dense and in intimate contact with the molybdenum. The dark regions in the sapphire are believed to be a crystal

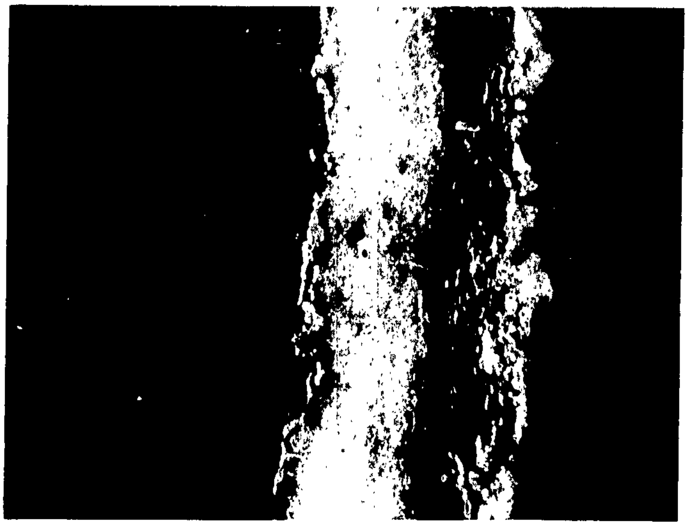

Molybdenum - Plasma-Sprayed Alumina -
Plasma-Sprayed Molybdenum Surfaces

(Magnification 138X - Oblique Illumination)

FIGURE 14 - PHOTOGRAPH OF ALUMINA-MOLYBDENUM STRUCTURE

Molybdenum - Cast Sapphire - Molybdenum Interfaces

The dark regions indicate a phase transformation from slow cooling.

(Magnification 194X - Direct Illumination)

FIGURE 15 - PHOTOGRAPH OF THE CROSS SECTION OF THE CAST-SAPPHIRE STRUCTURE

phase transformation produced by slow cooling. They can be eliminated by more rapid cooling. .

Extensive study by x-ray radiography was made to determine the soundness of the cast structure as a method of non-destructive testing. However, the results were not conclusive. The absorption coefficient was too small and the depth of the alumina too thin to detect flaws. However, an ultrasonic flaw detector has been acquired which was able to detect small voids. The flaws were confirmed when a section was made through the suspected regions. All new structures will be subjected to this non-destructive testing.

F Cesium Compatibility

During the past quarter additional tests were conducted in the same manner and in vessels of the same design as reported in the previous report. For the current report the greatest emphasis was directed toward finding a ceramic body which is not attacked by cesium, since the common metals used in converter construction had been evaluated earlier. The results of the individual tests will be discussed separately. Comparisons will be made for the effects at different temperatures.

The ceramic bodies which were tested are listed in Table III together with the stated minimum purity. Vendors consider the composition of their ceramic bodies are proprietary knowledge and will not disclose the materials which they use as fluxes in preparing the ceramics. However, it is general knowledge that silicon-oxide, magnesium-oxide and calcium-oxide are the most popular fluxes besides the occasional use of ferric-oxide, manganese-oxide and chrome-oxide.

1. Test Results at 370° Centigrade

Tests results were obtained for particular samples of ceramic bodies at

TABLE III

PURITY OF THE CERAMIC BODIES TESTED

Material	
Wesgo AL995	99.5% Al_2O_3
Wesgo AL300	97.6% Al_2O_3
Wesgo AL400	95.0% Al_2O_3
Silk City SC95D	95.0% Al_2O_3
Silk City SC98D	98.0% Al_2O_3
Coors AD96	96.0% Al_2O_3
Coors AD99	99.0% Al_2O_3
Alsimag 614	96.0% Al_2O_3
American Feldmuehle RK37Tr	99.+% Al_2O_3
Sapphire	100% Single Crystal Al_2O_3
Carborundum Boron Nitride	97.0% BN
*Minneapolis-Honeywell High MgO	
*Carborundum MgO #0340	
*Carborundum MgO #0333	

*There are no stated purities

370° Centigrade in liquid and vapor cesium at a pressure of 10 millimeters of mercury for 1000 hours. The results for the vapor attack are summarized in Table IV while the results in the liquid test are summarized in Table V. In general, it may be stated that liquid cesium attack is more severe than vapor cesium attack. All of the ceramic bodies but the RK37Tr, MgO #0340 and AD96 were stained by cesium vapor. Part of the surface of the Silk City ceramics (SC95D and SC98D) were also stained. This is shown in the micrograph Figure 16. Because of the nature of this local staining, it may be concluded that there are contaminants on the surface which initiated the attack. There was no change in the structure of the ceramic beneath the surface which could be associated with the staining of the surface. Two photomicrographs of these surface stains are shown in Figure 17 for two other bodies than the Silk City. Therefore, it may be concluded that at 370° Centigrade in vapor Silk City bodies SC98D and SC95D, Alsimag 614, American Feldmuehle RK37Tr, Carborundum MgO #0340, Wesgo AL995 and Coors AD96 are not grossly attacked althrough, as mentioned earlier, their surfaces are stained. Carborundum MgO #0333, Coors AD99, Minneapolis-Honeywell High MgO, Frenchtown 17225, are all attacked by cesium vapor as illustrated by a change in weight. The nature of the attack will be described more fully in the latter portion of this report where the attack is more severe.

The results in liquid cesium are the same as for vapor except that Carborundum MgO #0340 was stained on the surface and the change in weight for those bodies attacked was slightly greater.

In addition to the testing of ceramic bodies, three metals were evaluated which might potentially be incorporated in brazing alloys. Rhenium, Iridium and Palladium were tested and none were attacked by either liquid or vapor cesium at 370° Centigrade.

TABLE IV

CESIUM COMPATIBILITY AT 370° CENTIGRADE

VAPOR ATTACK

Material	Percent Weight Change	Description
Silk City SC98D	0%	Spots of gray on surface but no evidence of diffusion into the body.
Silk City SC95D		
Carborundum Boron Nitride		Sample disintegrated on life test when pinch-off opened.
Alsimag 614	0%	Surface light gray.
American Feldmuehle RK37Tr	0%	Surface remained white.
Carborundum MgO #0340	0%	Surface remained white.
Carborundum MgO #0333	-1. 94%	Gray
Coors AD99	0. 53%	Light gray with local dark gray areas.
Minneapolis-Honeywell High MgO	+0. 06%	Light gray.
Frenchtown 17225	+0. 26%	
Wesgo AL995	0%	Light gray surface.
Coors AD96	0%	Light gray in vapor.
Rhodium	0%	Surface remained metallic.
Iridium	1%*	Surface remained metallic.
Palladium	0%	Surface remained metallic.

*Change in weight was approximate due to minute size of sample.

TABLE V

CESIUM COMPATIBILITY AT 370° CENTIGRADE

LIQUID ATTACK

Material	Percent Weight Change	Description
Silk City SC98D	0%	Spots of gray on surface but no evidence of diffusion into the body.
Silk City SC95D		
Carborundum Boron Nitride		Sample disintegrated on life test when pinch-off opened.
American Feldmuehle RK37Tr	0%	No surface staining.
Carborundum MgO #0340	0%	Surface very lightly stained.
Carborundum MgO #0333	-2.22%	Dark gray.
Coors AD99	+0.192%	Light gray and local attack.
Minneapolis-Honeywell High MgO	+0.34%	Dark gray.
Frenchtown 17225	+0.29%	
Wesgo AL995	-0.06%	Light gray surface.
Wesgo AL300	0%	Remained white.
Coors AD96	+0.03%	Light gray.
Alsimag 614	0%	Light gray.
Rhodium	0%	Surface remained metallic.
Iridium	1%	Surface remained metallic.
Palladium	0%	Surface remained metallic.

SC98D ceramic after 1000 hours in cesium vapor at 370° Centigrade and 10 millimeters of mercury. Note dark gray region along upper half of sample.

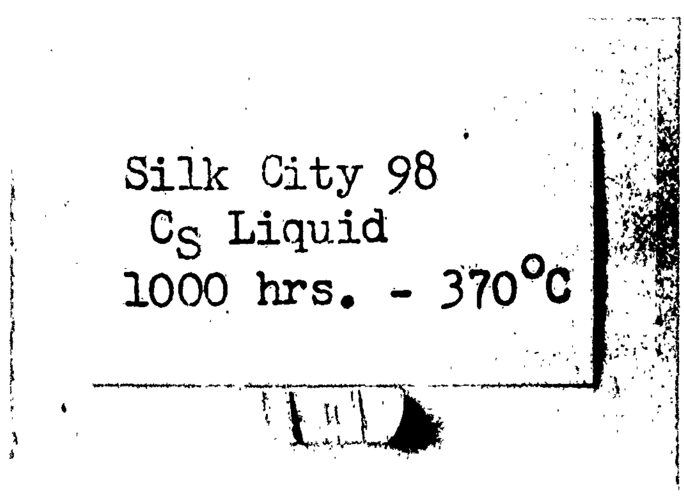

SC98D ceramic after 1000 hours in cesium liquid at 370° Centigrade. Note gray region in cut.

FIGURE 16 - EFFECTS OF CESIUM ON SC98D CERAMIC

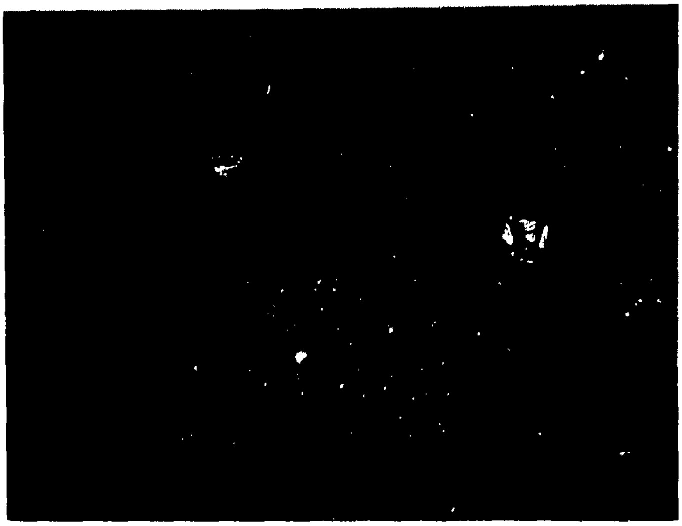

AL300 ceramic after 1000 hours in cesium liquid at 370° Centigrade. Staining is local and probably due to surface contaminants.

(Magnification 138X)

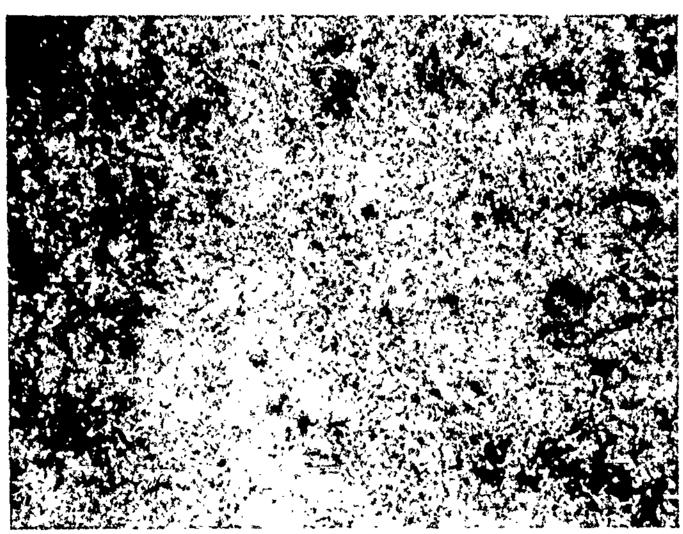

AL995 ceramic after 1000 hours in cesium liquid at 370° Centigrade. Surface was darkened to gray.

(Magnification 138X)

FIGURE 17 - EFFECTS OF LIQUID CESIUM ON AL300 AND AL995 CERAMICS

2. Test Results at 750° Centigrade

The results observed in testing the ceramic for 1000 hours at 750° Centigrade in cesium vapor at 10 millimeters of mercury pressure were more dramatic and enlightening as to the mechanism of attack. Table VI is a summary of the results. All of the bodies tested were attacked except the two Silk City bodies SC98D and SC95D. However, as described in the 370° Centigrade tests, the surface was darkened locally although no change was observed in the weight of the sample nor its structure.

The two ceramics most severely attacked were Frenchtown 17225 and Alsimag 614. A microphotograph of the Alsimag 614 is shown in Figure 18. These two bodies were extensively cracked throughout by induced strain from the diffusion of cesium into it. These cracks followed the isostatic planes in pressing the ceramic.

The next most severely attacked ceramic was the AL995 body. A photomicrograph of its structure is in Figure 19. It should be noted that the structure is very coarse and all of the attack occurred intergranularly in the region containing the flux. Such a structure is weakened considerably.

The next most severely attacked samples were American Feldmuehle RK37Tr, Boron Nitride, Carborundum MgO #0340 and MgO #0333. The cesium diffused throughout the bodies but did not induce enough strain to fracture the bodies. However, it was enough to make it impossible to make a cross section in some cases. The diffusion throughout the body was confirmed by a uniform graying of the structure from its edge to center when the samples were cut in half.

The ceramic bodies which were mildly attacked were Coors AD96, Coors AD99, Wesgo AL300 and Wesgo AL400. The structure in Figure 20 is typical of the cross section of these bodies. It is very easy to

TABLE VI

CESIUM COMPATIBILITY AT 750° CENTIGRADE -
10 MILLIMETERS OF PRESSURE

Material	Percent Weight Change	Description
Wesgo AL995	+0.21%	Dark gray throughout.
Coors AD96	+0.053%	Light gray on surface and to a depth of 0.015 inch.
Wesgo AL300	+0.96%	Dark on surface and to a depth of 0.020 inch.
Silk City SC95D	0%	Spots of gray on surface but no evidence of diffusion into the body.
Silk City SC98D		
Alsimag 614	+4.1%	Dark gray throughout the body, badly cracked.
Frenchtown 17225	+5.6%	Dark gray throughout the body, badly cracked.
Carborundum Boron Nitride		Surface became flaky.
American Feldmuehle RK37Tr	+0.65%	Surface light gray and diffused throughout body.
Minneapolis-Honeywell High MgO	+0.42%	Surface white.
Carborundum MgO #0340	0.25%	Surface gray and diffused throughout body.
Wesgo AL400	1.2%	Darkened on surface and diffused to a depth of about 0.020 inch.
Coors AD99	0.6%	Darkened on surface and diffused to a depth of about 0.010 inch.
Carborundum MgO #0333	2.5%	Disintegrated when attempting to analyze.

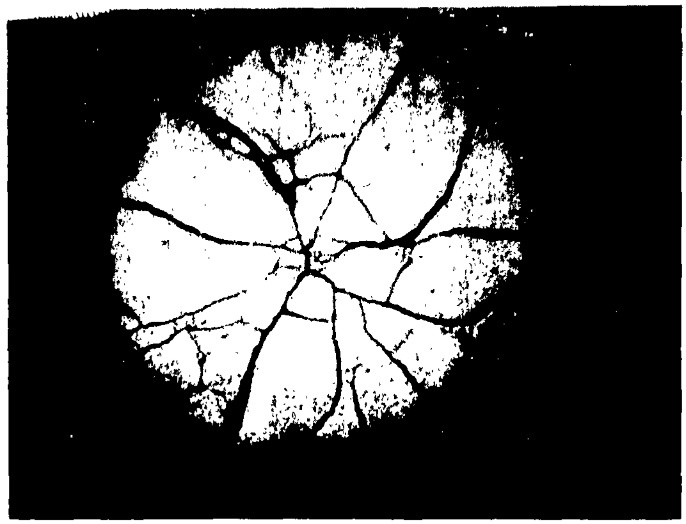

Cross section of 1/4 inch diameter test rod of Alsimag 614 ceramic. Note extensive cracking by the induced strain from the diffusion of cesium into it.

FIGURE 18 - EFFECTS OF CESIUM VAPOR AT 750° CENTIGRADE ON ALSIMAG 614 CERAMIC

Note intergranular penetration of the cesium

(Magnification 138X)

FIGURE 19 - EFFECTS OF CESIUM VAPOR AT
750° CENTIGRADE ON AL995 CERAMIC

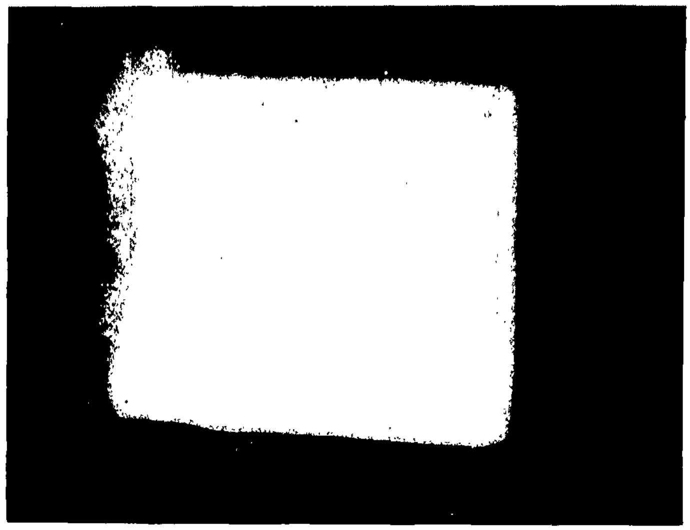

Note the depth to which cesium diffused by the discoloration of the ceramic

FIGURE 20 - EFFECTS OF CESIUM VAPOR AT 750° CENTIGRADE ON AL300 CERAMIC

distinguish the depth to which the cesium has diffused. When these samples are examined at a higher magnification the gray region cannot be easily identified as indicated by the micrograph in Figure 21. The only difference between the original matrix and attacked area appears to be an increase in the amount of intercrystalline phase near the surface.

In the case illustrated, the structural difference is rather clear and definitely shows that mechanism of attack is intergranular. However, it is impossible to observe changes within the intergranular phase other than an increase in its volume. Therefore, when the attack becomes less severe it is more difficult to observe structural changes. For this reason the greatest emphasis was applied to an observable change in weight. Since the change in weight is related to the surface area from which the diffusion starts a direct comparison could not be made because of the differences in the sample geometry.

Cross sections of the Silk City SC98D body are shown in Figure 22. There is no discoloration of the ceramic body to any observable depth and since there was no change in weight of the ceramic tested, it was concluded there was no attack by the cesium.

3. Test Results at 1200° Centigrade

Two ceramics were tested at 1200° Centigrade with a cesium pressure of 10 millimeters of mercury for 1000 hours. They are AL995 and sapphire and the results are summarized in Table VII. These samples were metalized and brazed to the emitter structure of a converter, Type A-1194. In the case of the sapphire, metalizing was very difficult. During the test, whiskers grew on the sample in the region where excess metalizing was applied. A photograph of these whiskers is shown in Figure 23. However, on cross-sectioning the sapphire no bulk attack was observed and it was concluded that sapphire was resistant to cesium attack.

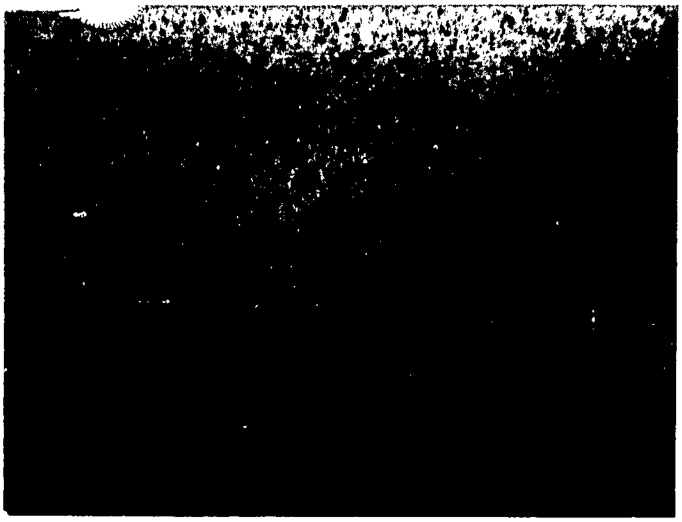

Note the graying due to the growth
of the intercrystalline phase

FIGURE 21 - EFFECTS OF CESIUM VAPOR AT
750° CENTIGRADE ON AL300 CERAMIC

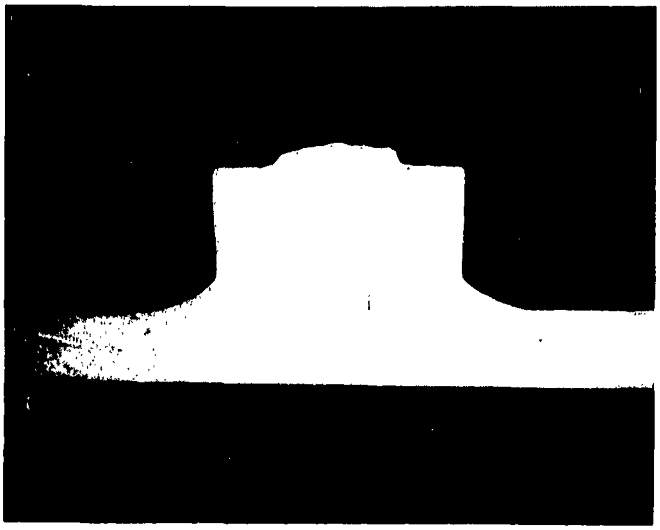

(Magnification 10X)

There appears to be no attack by cesium

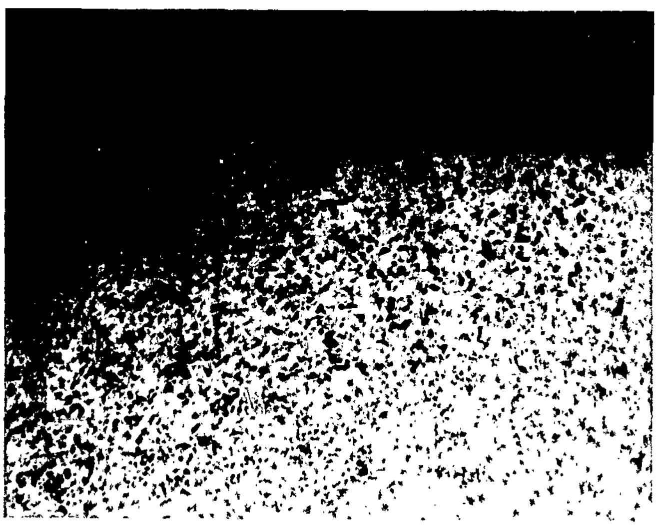

(Magnification 138X)

FIGURE 22 - EFFECTS OF CESIUM VAPOR AT 750° CENTIGRADE ON SC98D CERAMIC

TABLE VII

CESIUM COMPATIBILITY AT 1200° CENTIGRADE WITH CESIUM PRESSURE 10 MILLIMETRS FOR 1000 HOURS

Material	Description
Wesgo AL995	Attacked less than at 750° Centigrade.
Sapphire	No gross attack to sample was observed except in the region of metalizing.

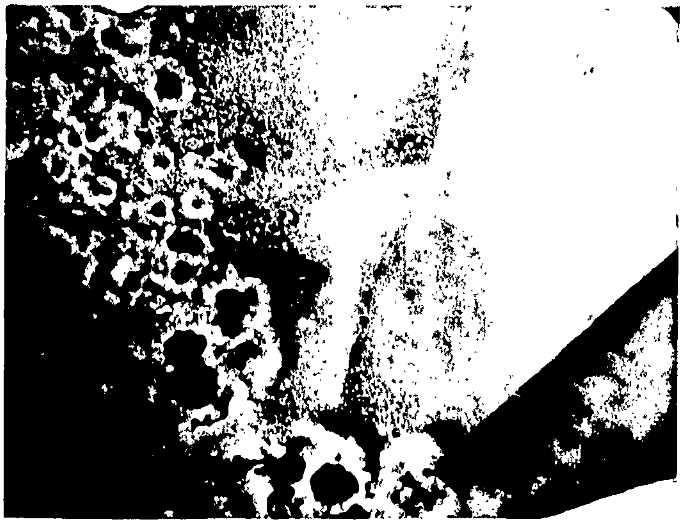

The edge of the sapphire sample shows whiskers
which grew because of excess metalizing

FIGURE 23 - EFFECTS OF CESIUM VAPOR AT
1200° CENTIGRADE ON SAPPHIRE SAMPLE

The other sample tested was Wesgo AL995 and a cross section if it is shown as Figure 24. It was attacked, but in comparing this photomicrograph with that in Figure 19, it will be noticed that the attack by the cesium vapor is less severe. The crack appearing in the sample was probably caused by the difference in coefficient of expansion during brazing and by the large area of the braze joint. Cracking was also observed in the sapphire sample for this reason.

The compatibility of cesium with the materials tested are summarized in Tables VIII and IX. Table VIII shows the resistance of material to attack by liquid cesium and Table IX shows the resistance of materials to attack by cesium vapor at a cesium pressure of 10 millimeters of mercury. If a material was found to have good resistance at a given temperature, it was considered to have good resistance at all lower temperatures and equal or lower cesium pressure. If a material was found to have poor or limited resistance at a given temperature, then it was considered to have poor or limited resistance at all higher temperatures.

In general, it may be stated that all the ceramic bodies tested except the two Silk City bodies SC95D and SC98D are attacked by cesium vapor and liquid when tested to temperatures of 750° Centigrade. Only Wesgo AL995, AL400, AL300, Alsimag 614, American Feldmuehle RK37Tr and Carborundum MgO #0340 are good to temperatures of 370° Centigrade. However, considering the nature of failure at 750° Centigrade, their use should be restricted at this temperature. It is conceivable that observable changes would be apparent if the hours of testing were extended. Sapphire was exceptionally resistant to attack but until a metalizing technique is developed which incorporates only compatible materials, sapphire cannot be considered a useful construction material.

Note the attack is less severe than
in Figure 19 (750° Centigrade)

(Magnification 138X)

FIGURE 24 - EFFECTS OF CESIUM VAPOR AT
1200° CENTIGRADE ON AL995 CERAMIC

TABLE VIII

THE RESISTANCE OF MATERIALS TO ATTACK BY CESIUM LIQUID

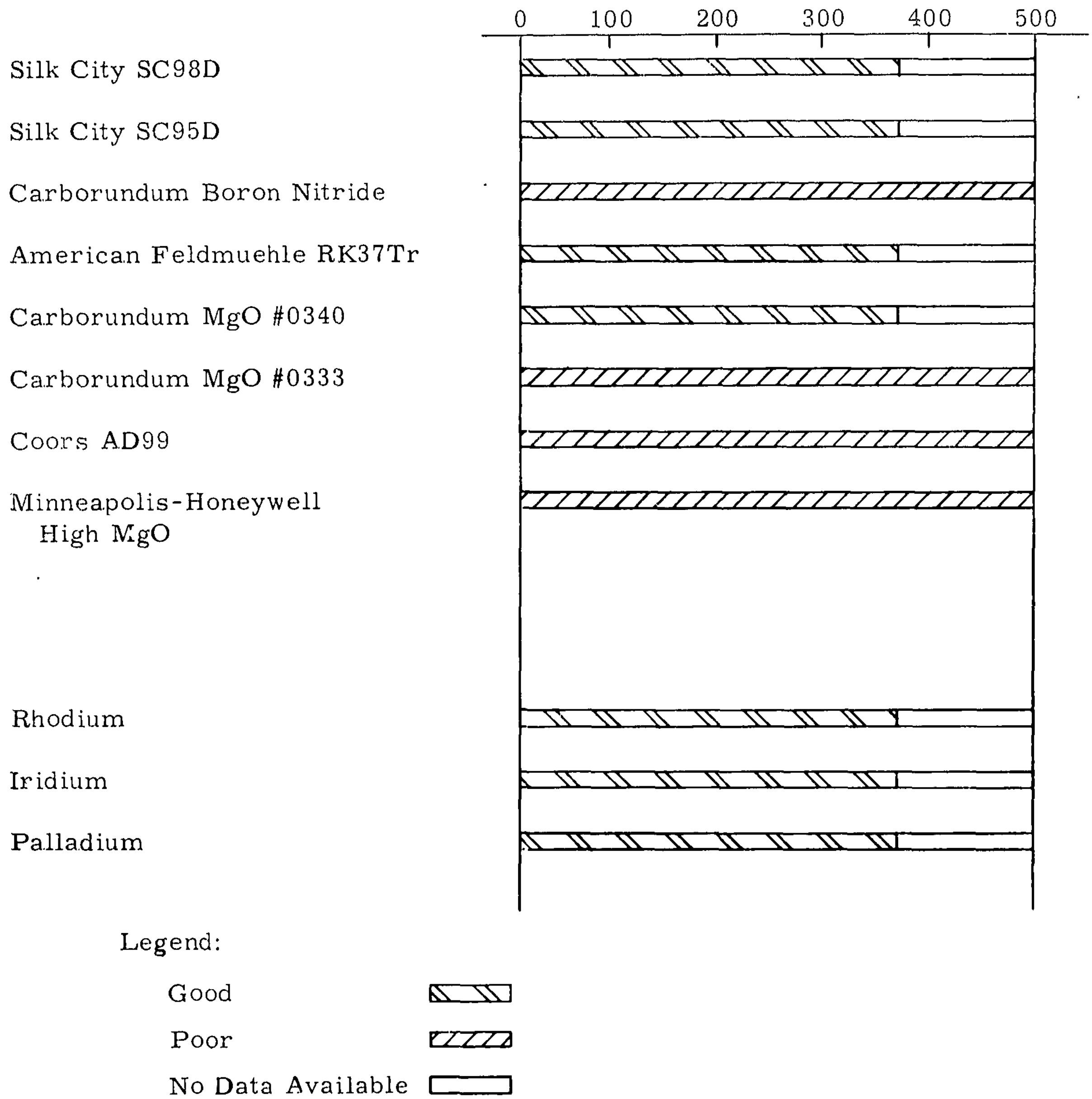

TABLE IX

RESISTANCE OF MATERIALS TO ATTACK BY CESIUM VAPOR AT A CESIUM PRESSURE OF 10 MILLIMETERS

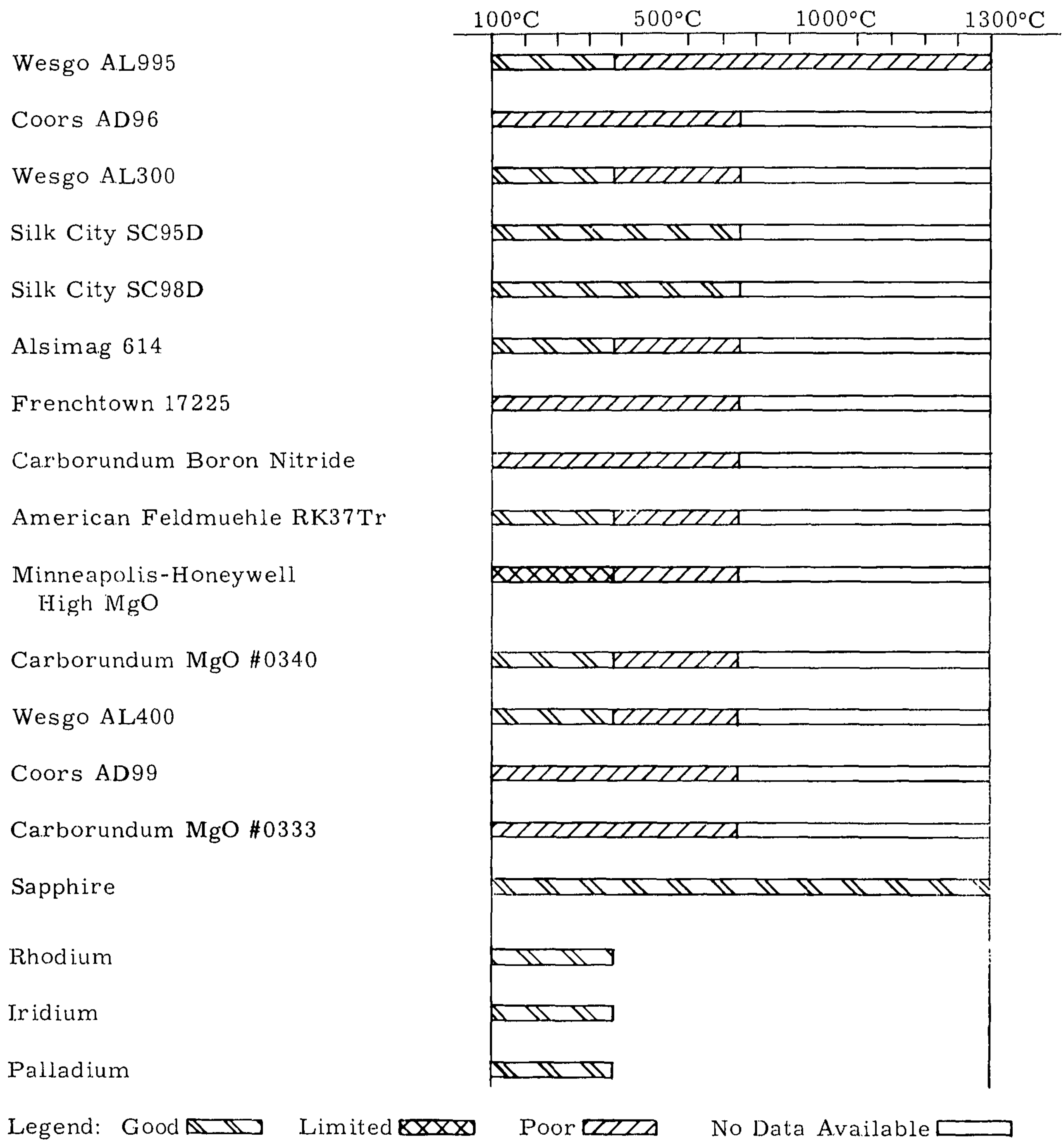

It was also concluded although the experimental evidence is general, that a fine grain alumina is more resistant to cesium attack than a coarse grain alumina, e. g. compare AL995 to AD99 where the cesium completely diffused throughout the AL995 but only penetrated 0. 010 for AD96 (Table VI) when tested at 750° Centigrade. This is believed to be a result that the mean free path for intergranular diffusion is shorter for the fine grain material.

The interaction of the material tested with liquid cesium (Table VII) follows the trends observed for vapor corrosion, however, the corrosion effects are generally more pronounced.

The metals, Rhenium, Iridium and Palladium showed resistance to cesium attack in the liquid and vapor phase when tested at 370° Centigrade.